Journal of Photochemistry and Photobiology A: Chemistry 216 (2010) 201–208

Contents lists available at ScienceDirect

Journal of Photochemistry and Photobiology A: Chemistry

journal homepage: www.elsevier.com/locate/jphotochem

N-doped TiO_2 by low temperature synthesis: Stability, photo-reactivity and singlet oxygen formation in the visible range

Christophe Cantau, Thierry Pigot, Jean-Charles Dupin, Sylvie Lacombe*

UMR CNRS 5254, Université de Pau et Pays de l'Adour, Institut Pluridisciplinaire de Recherche sur l'Environnement et les Matériaux (IPREM-ECP), Hélioparc, 2 rue du Président Angot, 64053 Pau cedex 9, France

ARTICLE INFO

Article history:
Available online 7 August 2010

Keywords:
N-doped TiO_2
Photo-oxidation
Visible light
Singlet oxygen

ABSTRACT

N-doped TiO_2 (NDTs) were prepared by sol–gel synthesis at low temperature starting from nanocolloidal TiO_2 and triethylamine according to well-known procedures. Diffuse reflectance UV (DRUV) spectroscopy showed a shift of the absorption to the visible range, while diffuse reflectance IRFT (DRIFT) evidenced the presence of a chemisorbed complex involving triethylamine. Powder XRD showed the sole formation of anatase polymorph of TiO_2 while XPS indicated successful incorporation of nitrogen. Our data are globally consistent with previous literature results, but emphasize the low thermal and photochemical stability of the nitrogen complex under air. Di-*n*-butylsulfide photo-oxidation in acetonitrile solution was successfully carried out under irradiation at 420 and 350 nm. The reaction rates were slower under visible light and the product distribution was very dependent upon the wavelength. Our results are discussed in parallel with the literature data assuming the favoured formation of singlet oxygen under visible light.

1. Introduction

The development of semi-conductors able to use visible light has been a field of growing interest during the last years, in order to carry out oxidation/mineralization reactions under "green chemistry" conditions, using oxygen or air as reactant. A smart approach is the modification of the overwhelmingly used photocatalyst, titanium dioxide (TiO_2), to shift its absorption spectrum (band gap 3.2 eV) towards the visible range. Different synthetic methods are currently studied: coupling with a photosensitizer or with another narrow band-gap semi-conductor which absorbs in the visible range, doping with metal impurities, preparing oxygen deficient TiO_2 and doping TiO_2 with non-metal atoms (anion doping). All these methods were recently reviewed by Fujishima et al. [1].

Among anion doping, incorporation of nitrogen atoms is the most studied, and the elaboration, characterization and photocatalytic activity of N-doped TiO_2 (NDT) were addressed in many recent papers. The synthesis of NDT as films or powders was carried out according to two main methods: sputtering and implantation techniques under high temperature synthesis (HTS) [2–13] and low temperature synthesis (LTS) [14–29]. In HTS methods, either the sputtering of a nitrogen gas (NH_3, N_2, etc) at high temperature on a TiO_2 target, or calcination of a titanium precursor ($TiCl_4$ or a layered titanate) with a nitrogen source (ammonium salt or ammonia for example) is described [30,31]. LTS methods are based on the reaction of a nanocolloïdal solution of TiO_2 with nitrogen containing organic compounds like amines. Gole et al. initiated this method and in the original paper [14], the active material was obtained without any calcination step contrary to preparations recently described by Ihara et al. [32], Sakhtivel et al. [24], and Kobayakawa et al. [33].

The photocatalytic activity of NDTs was evaluated by different reactions in solution and in the gas phase. The pioneer work of Asahi et al. demonstrated an actual improvement relative to conventional TiO_2 on the photodegradation of methylene blue and gaseous acetaldehyde under visible light [2]. However the bleaching of methylene blue on NDTs can also occur through other mechanisms (*i.e.* photosensitized formation of singlet oxygen). Acetone, ethylene [34], propan-2-ol [9], trichloroethylene [35], toluene [36] were also successfully oxidized by NDTs at the gas–solid interface. The results of photocatalytic tests in aqueous solution were more contrasted. Kisch and co-workers [24] reported that NDTs photo-oxidized 4-chlorophenol up to mineralization under visible light whereas Mrowetz et al. reported that the holes photogenerated by irradiation of NDTs could not oxidize $HCOO^-$ anion and that the catalyst prepared at low temperature suffered bleaching under UV irradiation [23]. It appears that "the preparation history, which dictates the types and level of nitrogen doping and the concentration of oxygen vacancies greatly influences the photoactivity" [1].

The origin of the photoactivity of NDTs was extensively discussed: the formation of $HO^\bullet$ was questioned [23], but the production of superoxide radical anion $O_2^{\bullet-}$ was not. Solid-sate NMR measurements combined with time-resolved diffuse reflectance (TDR) spectroscopy also provided direct evidence of ethylene glycol

* Corresponding author. Tel.: +33 559 407 579; fax: +33 559 407 622.
E-mail address: sylvie.lacombe@univ-pau.fr (S. Lacombe).

1010-6030/$ – see front matter © 2010 Elsevier B.V. All rights reserved.
doi:10.1016/j.jphotochem.2010.08.004

degradation on NDT under visible light irradiation and suggested that the photocatalytic reactions of organic compounds adsorbed on the surface of $TiO_{2-x}N_x$ proceeded via the surface intermediates of the oxygen reduction or water oxidation, not via the direct reaction with h^+ trapped at the N-induced mid-gap level [37,38]. Singlet oxygen formation, already evidenced with TiO_2 [39,40], was also observed under visible irradiation with NDT [41–44].

In this work, we got interested in the low temperature elaboration and reactivity of a nitrogen modified TiO_2 for di-*n*-butylsulfide (DBS) oxidation in acetonitrile solutions. We focused on the soft chemical modification developed by Gole et al. [14]: nitrogen doping is carried out by contact between a nanocolloidal solution of TiO_2 and triethylamine (NEt_3) at room temperature.

2. Experimental

2.1. Preparation of (un)modified TiO_2 photocatalysts

The nanocolloidal solution was prepared by a sol–gel route starting with titanium isopropoxide ($Ti[OCH(CH_3)_2]_4$). A solution of 5 mL of $Ti[OCH(CH_3)_2]_4$ in 95 mL of isopropyl alcohol was introduced dropwise (*ca* 1 mL min^{-1}) under vigorous magnetic stirring in 900 mL of distilled water at pH 2.37 (adjusted by addition of HNO_3) at room temperature. An opalescent nanocolloidal solution of TiO_2 was thus obtained. The material obtained from this sol will be called in the following TiO_2-gel. For this gel, two populations of nanoparticles size were found by light diffusion technique: around 10 nm and around 70 nm (probably arising from nanoparticles agglomeration). The particles size measurement was made on a DL 135-45 apparatus developed by the IFP (French Petroleum Institute): the technique allows the size measurement of concentrated solutions which could be dense or opaque. This method is thus suitable for emulsions or nanocolloidal samples.

Starting from TiO_2-gel, two different NDTs were prepared according to the method described by Gole et al. [14]. The third sample was prepared from a nanocolloidal commercial TiO_2 powder (Degussa P25) reacted with triethylamine.

N-doping of each catalyst was carried out by contact with an excess of triethylamine (NEt_3) during a few days under room temperature conditions:

- Directly with the TiO_2 nanocolloidal solution (yellow NDT or NDT_y). 5 mL of the nanocollidal solution was reacted at room temperature under gentle stirring (the two solutions are not miscible) with 15 mL of NEt_3 until a yellow color appeared (~3 days). The mixture was then evaporated under vacuum and the yellow solid isolated at the end was further dried on a vacuum line (~10^{-2} mbar) for 4 h at room temperature.
- Starting from the dried extract of nanocolloidal solution (orange NDT, NDT_o) or from the commercial TiO_2 powder (Degussa P25) (brown TiO_2, NDT_b). The dry extract obtained by evaporation of the nanocolloidal solution under gentle stirring at 50 °C was carefully grounded in a mortar. 100 mg of this dry extract (for NDT_o) or 500 mg of the Degussa P25 TiO_2 powder (for NDT_b) and 3 mL or 15 mL respectively of NEt_3 were reacted at room temperature under gentle stirring (to avoid any deposition of the solid on the walls of the reactor) for at least 3 days until an orange color appeared for NDT_o or 6 days for NDT_b. NEt_3 was evaporated on a rotating evaporator and the orange or brown solid further dried as previously. Under these conditions, 132 mg of NDT_o and 590 mg of NDT_b were obtained.

After evaporation of triethylamine and drying under vacuum, three catalysts with different colors were obtained: NDT_y (yellow), NDT_o (orange) and NDT_b (brown) powders are shown in Fig. 1.

2.2. NDTs characterization methods

DRUV spectra of the powders were recorded on a Varian Cary 5 spectrometer with a 110 mm PTFE integrating sphere [45]. The reflectance spectra were corrected against a teflon standard reflectance spectrum.

DRIFT spectra were recorded on a Magna 560 Nicolet spectrometer flushed with dried air, with a resolution of 4 cm^{-1} after signal averaging of 200 scans. The DRIFT spectra at different temperatures were collected with a high temperature environmental chamber (HTEC from SPECTRA TECH Inc.) with diffuse reflectance accessory. This accessory is designed to obtain in situ DRIFT spectra at controlled elevated temperature and reduced pressure (6×10^{-2} bars). A wideband liquid nitrogen-cooled mercury cadmium telluride (MCT) detector was used.

Powder XRD patterns were recorded on an INEL diffractometer using a curved position-sensitive detector (INEL CPS 120) calibrated with $Na_2Ca_3Al_2F_{14}$ as standard. The monochromatic radiation applied was Cu Kα (1.5406 Å) from a long fine focus Cu tube operating at 40 kV and 35 mA. Scans were performed over the 2θ range from 5° to 115°. Accurate unit cell parameters were determined by a least squares refinement from data collected by the diffractometer. Basal spacing distances for the different samples analysed were determined from the position of the $d(0\,0\,3)$ reflection.

XPS analyses were performed on a Kratos Axis Ultra photoelectron spectrometer with a magnetic immersion lens to increase the solid angle of photoelectron collection from small analysis areas and to minimize the aberrations of the electron optics. A monochromatic and focused Al Kα radiation (1486.6 eV, spot dimensions of 700 μm × 300 μm) was operated at 450 W under a residual pressure of 5×10^{-9} mbar. The spectrometer was calibrated using the photoemission lines of Au ($Au4f_{7/2}$ = 83.9 eV, with reference to the Fermi level) and Cu ($Cu2p_{3/2}$ = 932.5 eV); for the $Au4f_{7/2}$ line, the full-width at half-maximum (FWHM) was 0.86 eV in the recording conditions. Charge effects were compensated by the use of a charge neutralization system (low energy electrons [typically 1.85 eV]) which had the unique ability to provide consistent charge compensation. All the neutralizer parameters remained constant during analysis. Peaks were then shifted to align adventitious carbon C 1s photoemission to 284.6 eV bonding energy. High resolution regions were acquired at constant pass energy of 40 eV. The XPS signals were analyzed by using a least squares algorithm and a non-linear

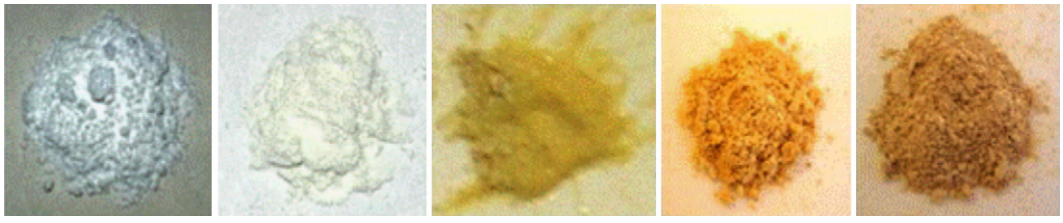

Fig. 1. Pictures of (a) commercial TiO_2 (Degussa P25), (b) TiO_2-gel, (c) yellow NDT (NDT_y), (d) orange NDT (NDT_o), and (e) brown NDT (NDT_b).

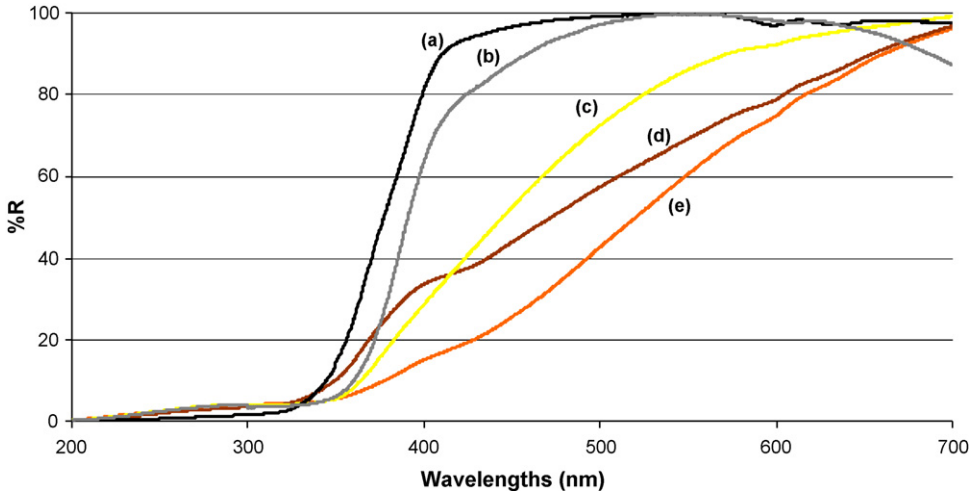

Fig. 2. DRUV spectra (%R) of (a) commercial TiO_2 (Degussa P25), (b) TiO_2-gel, (c) NDT_y, (d) NDT_b, and (e) NDT_o.

baseline. The fitting peaks of the experimental curves were defined by a combination of Gaussian (70%) and Lorentzian (30%) distributions.

2.3. Solution photo-oxidation

Photochemical experiments (5 h unless otherwise specified) were carried out by external irradiation in a Rayonet® photoreactor equipped either with four RPR-3500 Å lamps, or four RPR-4200 Å lamps (emission spectra in Supplementary Information, Figure S1). The reacting mixtures (5 mL of a 10^{-2} mol L^{-1} solution of di-n-butylsulfide in acetonitrile containing 15 mg of catalyst and cyclododecane as internal standard) were stirred and continuously bubbled with oxygen through a mass flow-meter (2 mL min^{-1}) during irradiation. Every hour, 10 μL of the solution was sampled and analyzed by gas chromatography (VARIAN 3900 with a FID detector, 15 m CP-Sil-5 Chrompack column, i.d.: 0.25 mm, coating 0.25 μm) in order to follow the reaction advancement.

3. Results

3.1. Characterization of NDTs

The coloration of the modified catalysts (Fig. 1) was in agreement with the bathochromic shift of the absorption spectra to the visible range, determined by diffuse reflectance UV (DRUV) spectra of the catalysts (Fig. 2).

The reflectance was maximum above 600 nm for NDT_y and 700 nm for NDT_o and NDT_b. From a recent review of the available data by Cheng and co-workers [31], the visible light absorption observed as a shoulder above 320 nm is characteristic of "the presence of localized states from N2p states as well as concomitant color centers in the band gap". Accordingly, these materials should be potentially active under visible light and their photocatalytic efficiency was checked.

The nature of the crystalline structure of these catalysts was determined by X-ray diffraction (XRD, Fig. 3). The most widely used TiO_2 photocatalyst, Degussa P25, is a 80/20 mixture of anatase and rutile (Fig. 3a), with clear lines at 25.3° and 39.00 (anatase, JCPDS card 21-1272) and 27.4 and 37.1° (rutile, JCPDS 21-1276). The large structure beyond 37° is an overlapping of anatase phase lines. The peaks obtained for TiO_2-gel (Fig. 3b) were much wider than those of commercial TiO_2, probably due to either a lesser crystallinity of the sample or to the presence of very small-sized particles. After calcination of the TiO_2-gel (temperature rise 10 °C min^{-1} up to 450 °C, then stationary for 3 h, Fig. 3c), a narrowing of the peaks width was observed, arising from an improvement of the crystalline structure. For both TiO_2-gel samples (before or after calcination), anatase was the main polymorph and no peak corresponding to the rutile structure is detected, contrary to commercial P25 TiO_2, while weak intensity lines at 30.8° could be associated with a brookite phase (JCPDS card 29-1360).

Diffractograms obtained for TiO_2-gel (Fig. 3b and c) and NDT_o (prepared from TiO_2-gel, Fig. 3d and e) before and after calcination show that the anatase polymorph (together with brookite in minor amounts) was preserved after modification with triethylamine. After calcination, once again, narrower peaks were obtained, indicating a higher crystallinity. A new unknown peak was observed at $2\theta = 18°$ on the NDT_o diffractogram (Fig. 3d) and could only be attributed to the modification arising from nitrogen doping. This peak was not observed for calcined NDT_o (Fig. 3e) diffractogram. The same observations could be made for NTD_b (Fig. 3f), although in this case no improvement of the crystallinity was noticed upon calcination, Degussa P25 TiO_2 being already well crystallized. Disappearance of the unknown peak suggests an evolution during calcination, confirmed by the discoloration of the catalyst after calcination at 450 °C for 3 h under air: the modification induced by nitrogen incorporation was not stable under these conditions. Moreover, as material drying under vacuum before calcination rules out the presence of physisorbed NEt_3 on the surface, it can be assumed that nitrogen atom was incorporated as an organics and formed a complex (unstable under calcinations in air) with titanium atoms on the surface.

Diffuse reflectance infra-red (DRIFT) spectra were recorded for NDT_o under vacuum (10^{-2} Torr) at different temperatures (Fig. 4). The presence of bands assigned to C–H stretching (2804, 2876, 2934 and 2963 cm^{-1}), even at high temperature, are consistent with the formation of an organometallic complex, not stable under air as suggested by the previous XRD diffractogram, but stable under vacuum, and rules out the possible physisorption of triethylamine only weakly bound to TiO_2. This result was different from that of Gole et al. for the same type of doping: after drying of their doped sample, no trace of organic compounds was detected by infra-red spectroscopy [18].

The nature of doping and more particularly of nitrogen incorporation has been a lively debate and XPS data were extensively discussed [1,46,47]. General XPS spectra confirm the incorporation of nitrogen in the doped catalysts, NDT_o and NDT_b (Figure S1 and S2). Expanded view of the N 1s region of the XPS spectra of TiO_2-gel, NDT_o and NDT_b before and after calcination are

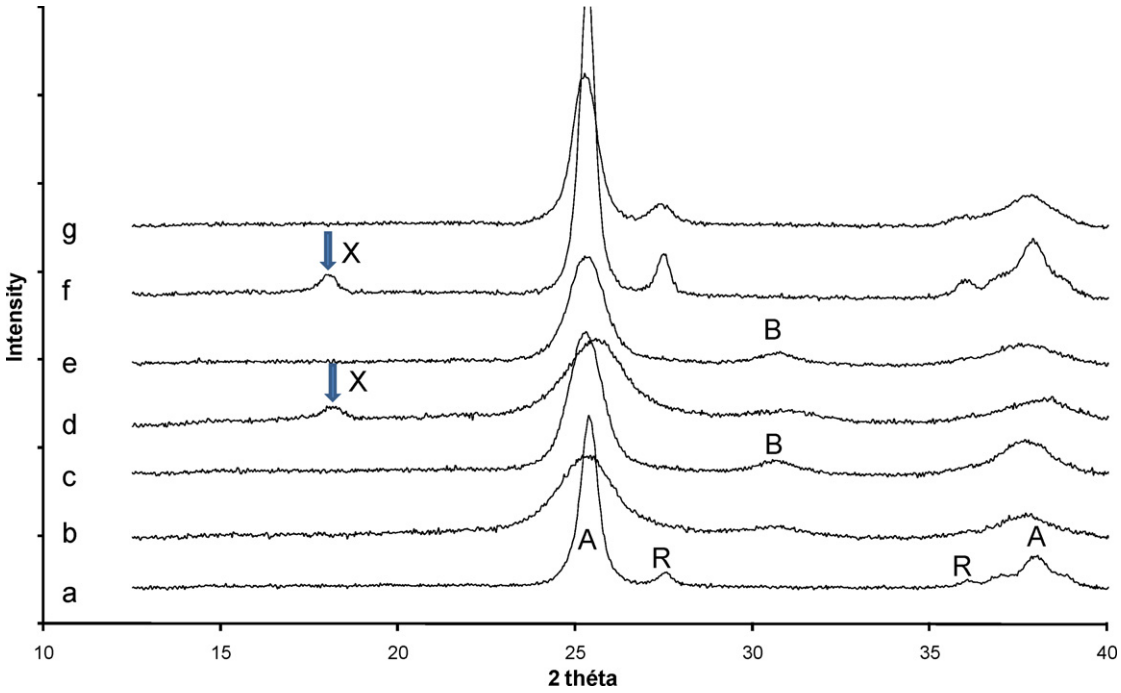

Fig. 3. Diffractograms of (a) commercial TiO_2 (Degussa P25), (b) TiO_2-gel, (c) calcinated TiO_2-gel, (d) NDT_o. (e) calcinated NDT_o, (f) NDT_b, and (g) calcinated NDT_b (A for anatase, R for rutile, B for brookite).

shown in Fig. 5. The nitrogen band was different for the two modified catalysts. As shown below, the high resolution N 1s peak was deconvoluted in three bands for NDT_o, but only in two bands for NDT_b (Fig. 6).

The analysis of high resolution spectra of Ti2p of all the samples (Supplementary information, Figure S3) confirmed the sole presence of titanium as TiO_2 ($Ti2p_{3/2}$ band at 458.4 eV and distance with $Ti2p_{1/2}$ peak about 5.7 eV).

On the core peak O 1s (Fig. 7), oxygen was observed under two different forms. The first band at 529.2 eV was attributed to a reduced form corresponding to oxygen atoms bound to titanium atoms (characteristic of TiO_2). The atomic ratio deduced from $Ti2p_{3/2}$/O 1s (529.2 eV) peaks was in the range 0.5 for all the samples, in agreement with TiO_2 formula. The second band around 531,4 eV was intense for uncalcined TiO_2-gel (23 at.%) and dropped to 7% for calcined TiO_2-gel and 6% for TiO_2 P25. This difference could only be assigned to the high ratio of hydroxyl groups on TiO_2-gel surface which dropped upon calcination.

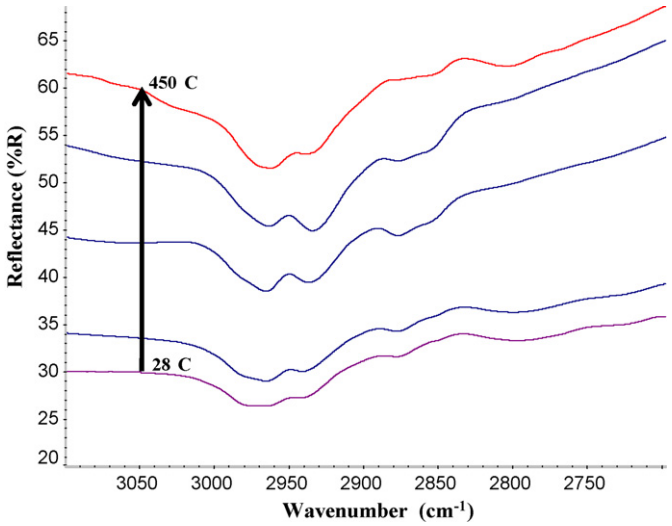

Fig. 4. DRIFT spectra of NDT_o under vacuum between 28 °C and 450 °C.

According to numerous XPS data recently reviewed, the N 1s core peak exhibits a different band structure, depending on the synthesis method [1,47]. The NDTs prepared by HTS method generally lead to the presence of a pattern of N 1s peak at 396 eV attributed to a nitrogen atom in a Ti–N environment, which is generally assigned to substitutional N for lattice O atoms. On the contrary, the LTS method commonly yields a NDT signal at 401.3 eV, attributed to interstitial nitrogen [47].

As already mentioned, the nitrogen high resolution spectra were different for NDT_o and NDT_b. From the peak integration of N 1s region (Fig. 5), the atomic concentration of nitrogen on the surface could be estimated: 4.4 at.% for NDT_o and of 3.3 at.% for NDT_b. After calcination, it dropped to 0.4 at.% for NDT_b, in agreement with the previous XRD assumptions. Two bands at 399.5 and 401.2 eV were observed for both doped materials. The exact state of nitrogen with its binding energy around 400 eV still needs further investigations even though many reports described such nitrogen species as O–Ti–N bonds [31]. The first band at 399.5 eV was recently assigned by Oropeza et al. to $(N0)_0'$, corresponding to interstitial nitrogen stabilized by a lattice O^{2-} to give NO^{2-} or $(N0)_0'$ in the Kröger–Vink notation [47]. According to the same authors, the second peak at 401.2 eV would correspond to NEt_4^+ contaminants left on the sample surface, by comparison with a binding energy of 401.5 eV reported for NH_4^+ species. In the NDT_o case, another band at 406.8 eV was also observed, characteristic of an oxidized nitrogen atom (surface NO_3^-). It was only observed on the doped nanocolloidal dried extract (NDT_o). These XPS results, like those of Oropeda et al., evidence a high sensitivity of the high resolution nitrogen XPS pattern of NDTs to the low temperature synthesis conditions (stirring time, presence of water, and solvent effect).

Most of these results are globally consistent with those published by Gole et al. [14], but bring about additional data:

- presence of an oxidized nitrogen atom (identified by its XPS peak at 406,8 eV) for NDT_o prepared from the dry extract of nanocolloidal TiO_2;

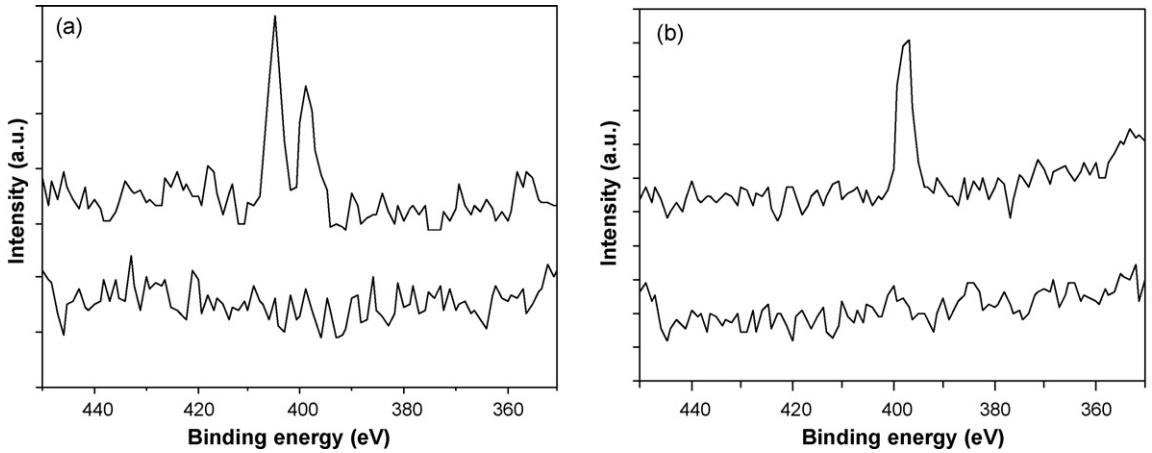

Fig. 5. Expanded view of the N1s region of the XPS spectra of a/upper curve: NDT_o, a/lower curve: TiO_2-gel, b/upper curve: NDT_b and b/lower curve: TiO_2-gel.

- presence of an un-assigned XRD peak sensitive to calcination under air for doped catalysts.
- presence of C–H stretching bands even at high temperature, consistent with the formation of an organometallic complex, not stable under air but stable under vacuum

On the other hand, with the chosen synthetic method (LTS), we confirm the absence of any peak at 396 eV (only observed for HTS preparation) assigned to a Ti–N bond [47].

3.2. Photoactivity of NDTs

The activity of these new photocatalysts for DBS oxidation in un-dried acetonitrile solution was checked both at 350 and at 420 nm, and compared to that of widely used Degussa TiO_2 P25. The evolution of DBS concentration with time for each photocatalysts at both wavelengths is presented in Fig. 8. The initial rates of DBS disappearance (apparent zero order kinetics determined from the experimental curves) and product distribution at 60% DBS consumption are summarized in Tables 1 and 2. The main oxidation products were *n*-butylsulfoxide (DBSO), *n*-

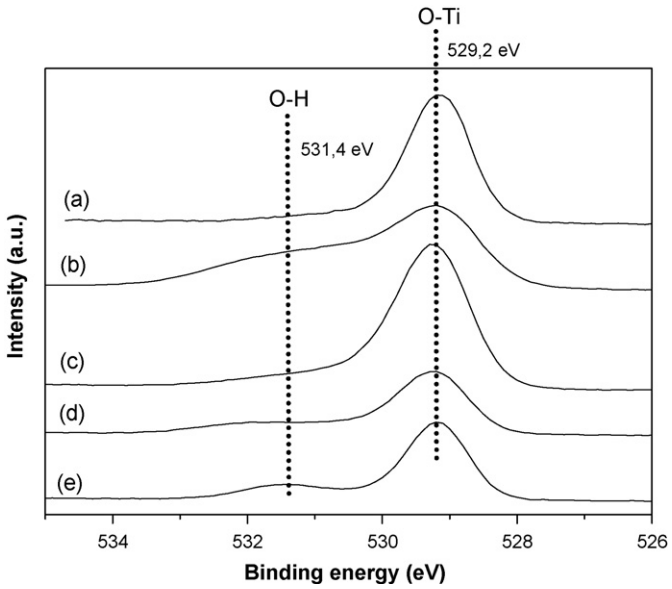

Fig. 7. High resolution XPS spectra of O1s peak for (a) commercial TiO_2 (Degussa P25), (b) TiO_2-gel, (c) calcined TiO_2-gel, (d) NDT_o, (e) NDT_b.

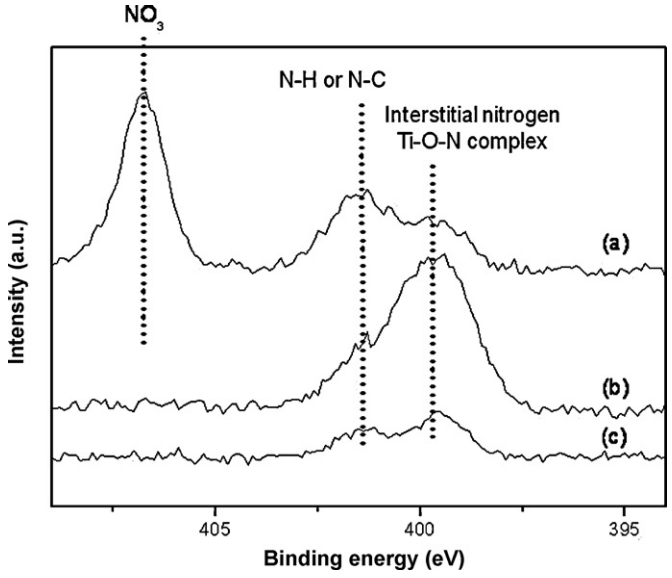

Fig. 6. High resolution XPS spectra of N1s peak for (a) NDT_o (b) NDT_b, (c) calcined NDT_b.

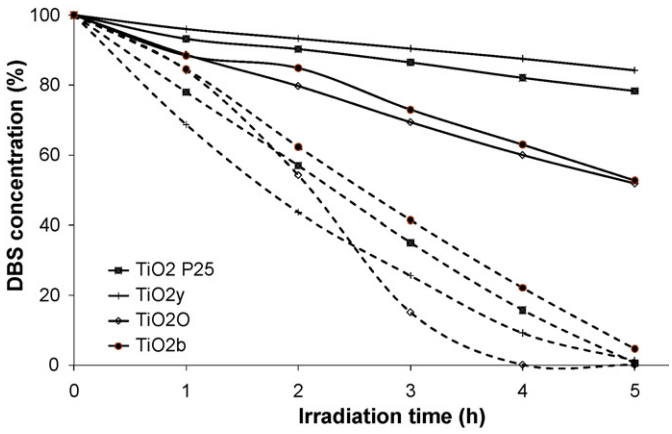

Fig. 8. Evolution of DBS concentration with irradiation time: 5 mL of a 10^{-2} mol L^{-1} solution of DBS in CH_3CN, 15 mg of photocatalyst, irradiation at 350 (dashed line) or 420 nm (straight line).

Table 1
Initial rate of BBS removal under irradiation at 350 nm or 420 nm of 10^{-2} mol L^{-1} DBS solutions in oxygenated CH_3CN.

	Initial rate of DBS removal (350 nm) (v_i, 10^{-3} mol l^{-1} h^{-1})	Initial rate of DBS removal (420 nm) (v_i, 10^{-3} mol l^{-1} h^{-1})
TiO_2 P25	2.3 ± 0.2	0.8 ± 0.1
NDT_y	3.7 ± 0.4	0.4 ± 0.1
NDT_o	1.8 ± 0.2	1.2 ± 0.1
NDT_b	2.2 ± 0.2	1.4 ± 0.1

butylsulfone ($DBSO_2$), di-*n*-butyldisulfide (DBDS), and *n*-butyl *n*-butanethiosulfonate ($DBSSO_2$).

At 350 nm, the initial rates are of the same order of magnitude for the four photocatalysts, with a noticeable slightly higher value for NDT_y (Table 1). This result indicates that nitrogen incorporation does not modify the photooxidizing properties of the catalyst at 350 nm. At 420 nm, DBS consumption with both TiO_2 P25 and NDT_y is much lower than at 350 nm. This result which could be expected with TiO_2 P25 is more surprising for NDT_y. For the two other photocatalysts, higher initial rates are obtained, although 1.5 times weaker than under 350 nm irradiation. To summarize, in spite of a lower activity under visible light than under 350 nm irradiation, NDT_o and NDT_b demonstrate significant photooxidizing properties for DBS oxidation in acetonitrile solution.

After 2 h under 350 nm irradiation, the products distribution depended on the catalyst and two sets of experiments could be distinguished (Table 2):

- those (NDT_y and NDT_o) where DBSO is the main oxidation product, while only very low amounts of di *n*-butyldisulfide are obtained (entries 2 and 3);
- those (TiO_2 P25 and NDT_b) with lower amount of DBSO and higher yields of DBDS and $DBSSO_2$ (entries 1 and 5).

It may be noted that acids (*n*-butanesulfonic acid and sulfuric acid) were detected as traces with all the catalysts except NDT_y, which also appeared as the most selective for DBSO.

The nature of the oxidation products is indicative of different mechanisms, *i.e.*

- type I by electron transfer and oxydo-reduction reactions leading to disulfide and acids after C–S bond cleavage,
- or type II with singlet oxygen addition to sulfide mainly leading to sulfoxide and sulfone [48].

From our results at 350 nm, it appears that type I mechanisms is the main oxidation pathway for TiO_2 P25 and NDT_m, while type II mechanism is predominant for NDT_o and NDT_y [49].

Under 420 nm irradiation, 60% DBS consumption was achieved within 5 h with NDT_o and NDT_b, while the reaction time was longer for NDT_y and P25 TiO_2. With the former photocatalysts, the products distribution is indicative of a type II reaction pathway, with a high selectivity for DBSO, as with NDT_o and NDT_y under 350 nm irradiation (entries 4 and 6).

It is worth noting that with NDT_b, different products distribution was observed depending on the irradiation wavelength (entries 5 and 6): higher DBSO selectivity is obtained at 420 nm (39.8%) than at 350 nm (23.1%), while DBDS yields decrease from 14.6% to 4.4%. At 420 nm, type II mechanism is probably the main reaction pathway, while type I reaction pathway is favored at 350 nm. For comparison, the same observation was made with TiO_2 P25 for a 20% DBS consumption after 5 h irradiation: DBSO is obtained in higher yields at 420 nm (18%) than at 350 nm (8%), whereas DBDS yield is higher at 350 nm (5% against less than 1% at 420 nm).

Additional experiments were also carried out for dimethylsulfide (DMS) oxidation in the gas phase on a previously described one-path reactor: dry synthetic air containing a known concentration of DMS continuously flowed on the irradiated catalyst at a controlled flow-rate [50]. For these experiments, the TiO_2 powders were deposited on a filter paper. Under 420 nm irradiation in dry air in a one-path experiment, DMS oxidation was negligible for all the modified catalysts and P25 TiO_2. However, it is important to mention that after 120 h of irradiation, discoloration of the materials was observed. This result implies a poor stability of the catalyst under irradiation in the presence of air.

4. Discussion

Starting from an already described low temperature synthesis of nitrogen doped TiO_2, this study confirmed the previous characterization of the NDTs, brought about some new data, checked their solution phase reactivity towards *n*-butylsulfide and gave some insights on their stability.

The synthetic method leads without calcination to the formation of crystallized TiO_2 in its anatase polymorph. A new band sensitive to calcination is however detected at small angle in the DRX pattern and is tentatively attributed to a surface complex between TiO_2 and triethylamine. Our XPS spectra confirm the lack of substitutional nitrogen atoms in the network (Ti–N bonds), characterized by their N 1s band at 396 eV, but appear more complex than those described in the original paper of Gole et al. [14], in agreement with recent results from Oropeza et al. [47]. The nitrogen pattern contains two or three bands, depending on the starting TiO_2 (TiO_2-gel or TiO_2 Degussa P25). A N 1s band at 406.2 eV, corresponding to an oxidized nitrogen (surface nitrate), is only observed for NDT_o, before calcination. The intensity of the bands at 399.5 and 401.2 eV drops upon calcination: their accurate assignment is not obvious, but an unstable surface complex between titanium and triethylamine is probably involved. From these results and from the discoloration of NDTs either after calcination or after visible irradiation in the presence of air, the formation of a sensitive surface complex may be assumed in agreement with FTIR data.

In order to characterize the photoactivity of the NDTs, an original test was carried out and gave some insights into oxidation mechanisms, which were shown to depend on the NDT and on

Table 2
Product distribution after irradiation at 350 nm or 420 nm of 10^{-2} mol L^{-1} DBS solutions in oxygenated CH_3CN (~60% DBS consumption).

Entry	Catalyst	Irradiation wavelength (nm)	DBS (%)	DBSO (%)	$DBSO_2$ (%)	DBDS (%)	$DBSSO_2$ (%)	Σ (%)
1	TiO_2 P25	350	40	17.2	1.2	12.4	4.6	75.4
2	NDT_y	350	40	54.5	4.1	0.8	0.6	100.0
3	NDT_o	350	40	30.6	0.7	3.4	–	74.7
4		420	43	34	1.1	1.2	1.4	81.0
5	NDT_b	350	40	23.1	1.6	14.6	3.4	82.7
6		420	45	39.8	0.6	4.4	–	89.4

DBSO: di *n*-butylsulfoxide; $DBSO_2$: di *n*-butylsulfone; DBDS: di *n*-butyldisulfide; $DBSSO_2$: *n*-butyl *n*-butanethiosulfonate

the irradiation wavelength. All the NDTs were reactive at 420 nm, although the oxidation rate of *n*-butylsulfide was slower than under irradiation at 350 nm. The product distribution strongly suggests that two mechanisms compete: singlet oxygen addition leading mainly to sulfoxide and sulfone, or radical mechanism via electron transfer species and photogenerated holes yielding high amounts of disulfide and thiosulfonate arising from C–S bond cleavage. Singlet oxygen mechanism is favored with NDTs at 420 nm. At 350 nm, disulfide formation is favored with the TiO_2 P25 based catalysts (modified or not), while singlet oxygen addition is more significant with the modified TiO_2 gels, NDT_y and NTD_o. These conclusions are in agreement with various literature results reporting the formation of singlet oxygen upon irradiation of TiO_2 [39,40]. It was recently demonstrated that modified N-doped TiO_2 do not react the same way with ethylene glycol under 350 or 460 nm irradiation, with 10 times slower reaction rate constants in the visible [38]. ESR experiments on N,S co-doped TiO_2 not only confirmed that hydroxyl radicals were not formed, contrary to superoxide radical anion $O_2^{\bullet -}$ which gave a strong signal, but that singlet oxygen was also observed [42,43]. Single molecule determination of airborne $^1O_2$ was more significant for NDT than for TiO_2 under visible illumination, while the same number of $^1O_2$ molecules were observed from both samples under UV light [44]. According to these authors, $^1O_2$ formation should arise from oxidation by the mid band-gap states holes of superoxide radical anion, $O_2^{\bullet -}$. Accordingly, as suggested by Majima, the photocatalytic reaction of *n*-butylsulfide adsorbed on the surface of TDN probably proceeds via surface intermediates issued from oxygen reduction (superoxide radical anion, $O_2^{\bullet -}$) but not via the direct reaction with photogenerated h^+ [38]. It is well known that superoxide anion is able to produce singlet oxygen in the presence of water [51]. Another possible assumption could be the direct photosensitization of ground state oxygen by the surface complex although, to the best of our knowledge, no such direct energy transfer was never reported.

5. Conclusion

N-doped TiO_2 (NDTs) prepared by sol–gel synthesis at low temperature starting from nanocolloidal TiO_2 and triethylamine according to published procedures were characterized by various methods. Our data are globally consistent with previous literature results, but emphasize the low thermal and photochemical stability of the nitrogen complex under air. Di-*n*-butylsulfide photo-oxidation in acetonitrile solution was successfully carried out under irradiation at 420 and 350 nm. The reaction rates were slower under visible light and the product distribution was very dependent upon the wavelength. Our results are discussed in parallel with literature data assuming the favored formation of singlet oxygen under visible light.

Acknowledgment

"Conseil Regional d'Aquitaine" funded CC and is greatly acknowledged.

Appendix A. Supplementary data

Supplementary data associated with this article can be found, in the online version, at doi:10.1016/j.jphotochem.2010.08.004.

References

[1] A. Fujishima, X. Zhang, D.A. Tryk, TiO_2 photocatalysis and related surface phenomena, Surf. Sci Rep. 63 (2008) 515–582.
[2] R. Asahi, T. Morikawa, T. Ohwaki, K. Aoki, Y. Taga, Visible-light photocatalysis in nitrogen-doped titanium oxides, Sciences 293 (2001) 269–271.
[3] M. Batzill, E.H. Morales, U. Diebold, Surface studies of nitrogen implanted TiO_2, Chem. Phys. 339 (2007) 36–43.
[4] J.M. Mwabora, T. Lindgren, E. Avenado, T.F. Jaramillo, J. Lu, S.E. Lindquist, C.G. Grandquist, Structure, composition, and morphology of photoelectrochemically active $TiO_{2-x}N_x$ thin films deposited by reactive DC magnetron sputtering, J. Phys. Chem. B 108 (2004) 20193–20198.
[5] O. Diwald, T.L. Thompson, T. Zubrov, E.G. Goralski, S.D. Walck, J.T. Yates, Photochemical activity of nitrogen-doped rutile TiO_2(1 1 1) in visible light, J. Phys. Chem. B 108 (2004) 6004–6008.
[6] H. Irie, S. Washizuka, N. Yoshino, K. Hashimoto, Visible-light induced hydrophylicity on nitrogen-substituted titanium dioxide films, Chem. Commun. 11 (2003) 1298–1299.
[7] Y. Nakano, T. Morikawa, T. Ohwaki, Y. Taga, Deep-level optical spectroscopy investigation of N-doped TiO_2 films, Appl. Phys. Lett. 86 (2005) 132104.
[8] M. Kitano, K. Funatsu, M. Matsuoka, M. Ueshima, M. Anpo, Preparation of nitrogen-substituted TiO_2 thin film photocatalysts by the radio frequency magnetron sputtering deposition method and their photocatalytic reactivity under visible light irradiation, J. Phys. Chem. B 110 (2006) 25266–25272.
[9] H. Irie, Y. Watanabe, K. Hashimoto, Nitrogen-concentration dependence on photocatalytic activity of $TiO_{2-x}N_x$ powders, J. Phys. Chem. B 107 (2003) 5483–5486.
[10] S.Z. Chen, P.Y. Zhang, D.M. Zhuang, W.P. Zhu, Investigation of nitrogen doped TiO_2 photocatalytic films prepared by reactive magnetron sputtering, Catal. Commun. 5 (2004) 677–680.
[11] V. Pore, M. Heikkil, M. Ritala, M. Leskel, S. Areva, Atomic layer deposition of $TiO_{2-x}N_x$ thin films for photocatalytic applications, J. Photochem. Photobiol. A: Chem. 177 (2006) 68–75.
[12] H. Li, J. Li, Y. Huo, Highly active TiO_2N photocatalysts prepared by treating TiO_2 precursors in NH_3/ethanol fluid under supercritical conditions, J. Phys. Chem. B 110 (2006) 1559–1565.
[13] S. Chen, X. Liu, Y. Liu, G. Cao, The preparation of nitrogen-doped $TiO_{2-x}N_x$ photocatalyst coated on hollow glass microbeads, Appl. Surf. Sci. 253 (2007) 3077–3082.
[14] J.L. Gole, J.D. Stout, C. Burda, Y. Lou, X. Chen, Highly efficient formation of visible light tunable $TiO_{2-x}N_x$ photocatalysts and their transformation at the nanoscale, J. Phys. Chem. B 108 (2004) 1230–1240.
[15] R. Bacsa, J. Kiwi, T. Ohno, P. Albers, V. Nadtochenko, Preparation, testing and characterization of doped TiO_2 active in the peroxidation of biomolecules under visible light, J. Phys. Chem. B 109 (2005) 5994–6003.
[16] X. Chen, C. Burda, Photoelectron spectroscopic investigation of nitrogen-doped titania nanoparticles, J. Phys. Chem. B 108 (2004) 15446–15449.
[17] X. Chen, Y. Lou, A.C.S. Samia, C. Burda, J.L. Gole, Formation of oxynitride as the photocatalytic enhancing site in nitrogen-doped titania nanocatalysts: comparison to a commercial nanopowder, Adv. Funct. Mater. 15 (2005) 41–49.
[18] S.M. Prokes, J.L. Gole, X. Chen, C. Burda, W.E. Carlos, Defect-related optical behavior in surface-modified TiO_2 nanostructures, Adv. Funct. Mater. 15 (2005) 161–167.
[19] M. Sathish, B. Viswanathan, R.P. Viswanath, C.S. Gopinath, Synthesis, characterization, electronic structure, and photocatalytic activity of nitrogen-doped TiO_2 nanocatalyst, Chem. Mater. 17 (2005) 6349–6353.
[20] C. Belver, R. Bellod, A. Fuerte, M. Fernandez-Garcia, Nitrogen-containing TiO_2 photocatalysts. Part 1. Synthesis and solid characterization, Appl. Catal. B: Environ. 65 (2006) 301–308.
[21] S. Sakthivel, H. Kisch, Photocatalytic and photoelectrochemical properties of nitrogen-doped titanium dioxide, Chem. Phys. Chem. 4 (2003) 487–490.
[22] T. Matsumoto, N. Iyi, Y. Kaneko, K. Kitamura, S. Ishihara, Y. Takasu, Y. Murakami, High visible-light photocatalytic activity of nitrogen-doped titania prepared from layered titania/isostearate nanocomposite, Catal. Today 120 (2007) 226–232.
[23] M. Mrowetz, W. Balcerski, A.J. Colussi, M.R. Hoffmann, Oxidative power of nitrogen-doped TiO_2 photocatalysts under visible illumination, J. Phys. Chem. 108 (2004) 17269–17273.
[24] S. Sakhtivel, M. Janczarek, H. Kisch, Visible light activity and photoelectrochemical properties of nitrogen-doped TiO_2, J. Phys. Chem. B 108 (2004) 19384–19387.
[25] T. Sano, N. Negishi, K. Koike, K. Takeuchi, S. Matsuzawa, Preparation of a visible light-responsive photocatalyst from a complex of $Ti4^+$ with a nitrogen-containing ligand, J. Mater. Chem. 14 (2004) 380–384.
[26] Z. Wang, W. Cai, X. Hong, X. Zhao, F. Xu, C. Cai, Photocatalytic degradation of phenol in aqueous nitrogen-doped TiO_2 suspensions with various light sources, Appl. Catal. B 57 (2005) 223–231.
[27] T. Ihara, M. Miyoshi, Y. Iriyama, O. Matsumoto, S. Sugihara, Visible-light-active titanium dioxide photocatalyst realized by an oxygen-deficient structure and by nitrogen doping, Appl. Catal. B 42 (2003) 403–409.
[28] S. Livraghi, M.C. Paganini, E. Giamello, A. Selloni, C.D. Valentin, G. Pacchioni, Origin of photoactivity of nitrogen-doped titanium dioxide under visible light, J. Am. Chem. Soc. 128 (2006) 15666–15671.
[29] Y. Liu, X. Chen, J. Li, C. Burda, Photocatalytic degradation of azo dyes by nitrogen-doped TiO_2 nanocatalysts, Chemosphere 61 (2005) 11–18.
[30] D. Li, H. Haneda, S. Hishita, N. Ohashi, Visible-light-driven N-F-codoped TiO_2 photocatalysts. 2. Optical characterization, photocatalysis, and potential application to air purification, Chem. Mater. 17 (2005) 2596–2602.

[31] G. Liu, L. Wang, C. Sun, X. Yan, X. Wang, Z. Chen, S. Smith, H. Cheng, G. Lu, Band-to-band visible-light photon excitation and photoactivity induced by homogeneous nitrogen doping in layered titanates, Chem. Mater. 21 (2009) 1266–1274.
[32] T. Ihara, M. Miyoshi, Y. Iriyama, O. Matsumoto, S. Sugihara, Appl. Catal. B 42 (2003) 403.
[33] K. Kobayakawa, Y. Murakami, Y. Sato, J. Photochem. Photobiol. A 170 (2005) 177.
[34] S. Kumar, A.G. Fedorov, J.L. Gole, Photodegradation of ethylene using visible light responsive surfaces prepared from titania nanoparticles slurries, Appl. Catal. B: Environ. 57 (2005) 93–107.
[35] K. Demeestere, J. Dewulf, T. Ohno, P.H. Salgado, H. Van Langenhove, Visible light mediated photocatalytic degradation of gaseous trichloroethylene and dimethyl sulfide on modified titanium dioxide, Appl. Catal. B: Environ. 61 (2005) 140–149.
[36] Y. Irokawa, T. Morikawa, K. Aoki, S. Kosaka, T. Ohwaki, Y. Taga, Photodegradation of toluene over $TiO_{2-x}N_x$ under visible light irradiation, Phys. Chem. Chem. Phys. 8 (2006) 1116–1121.
[37] T. Tachikawa, S. Tojo, K. Kawai, M. Endo, M. Fujitsuka, T. Ohno, K. Nishijima, Z. Miyamoto, T. Majima, Photocatalytic oxidation reactivity of holes in the sulfur- and carbon-doped TiO_2 powders studied by time-resolved diffuse reflectance spectroscopy, J. Phys. Chem. B 108 (2004) 19299–19306.
[38] T. Tachikawa, Y. Takai, S. Tojo, M. Fujitsuka, H. Irie, K. Hashimoto, T. Majima, Visible light-induced degradation of ethylene glycol on nitrogen-doped TiO_2 powders, J. Phys. Chem. B 110 (2006) 13158–13165.
[39] Y. Nosaka, T. Daimon, Y.A. Nosaka, Y. Murakami, Singlet oxygen formation in photocatalytic TiO_2 aqueous suspension, Phys. Chem. Chem. Phys 6 (2004) 2917–2918.
[40] K. Hirakawa, T.T. Hirano, Singlet oxygen generation photocatalyzed by TiO_2 particles and its contribution to biomolecule damage, Chem. Lett. 35 (2006) 832–833.
[41] I.C. Kang, Q.W. Zhang, S. Yin, T. Sato, F. Saito, Improvement of photocatalytic activity of TiO_2 under visible irradiation through addition of N-TiO_2, Environ. Sci. Technol. 42 (2008) 3622–3626.
[42] J.A. Rengifo-Herrera, K. Pierzchala, A. Sienkiewicz, L. Forro, J. Kiwi, J.E. Moser, C. Pulgarin, Synthesis, characterization, and photocatalytic activities of nanoparticulate N,S-codoped TiO_2 having different surface-to-volume ratios, J. Phys. Chem. C 114 (2010) 2717–2723.
[43] J.A. Rengifo-Herrera, K. Pierzchala, A. Sienkiewicz, L. Forro, J. Kiwi, C. Pulgarin, Abatement of organics and *Escherichia coli* by N,S co-doped TiO_2 under UV and visible light. Implications of the formation of singlet oxygen ($O\text{-}^1{}_{(2)}$) under visible light, Appl. Catal. B.: Environ. 88 (2009) 398–406.
[44] K. Naito, T. Tachikawa, M. Fujitsuka, T. Majima, Real-time single-molecule imaging of the spatial and temporal distribution of reactive oxygen species with fluorescent probes: Applications to TiO_2 photocatalysts, J. Phys Chem. C 112 (2008) 1048–1059.
[45] S. Lacombe, H. Cardy, N. Soggiu, S. Blanc, J.L. Habib-Jiwan, J.Ph. Soumillion, Diffuse reflectance UV–Visible spectroscopy for the qualitative and quantitative study of chromophores adsorbed or grafted on silica, Micropor. Mesopor. Mater. 46 (2001) 311.
[46] R. Beranek, H. Kisch, Tuning the optical and photoelectrochemical properties of surface-modified TiO_2, Photochem. Photobiol. Sci. 7 (2008) 40–48.
[47] F.E. Oropeza, J. Harmer, R.G. Egdell, R.G. Palgrave, A critical evaluation of the mode of incorporation of nitrogen in doped anatase photocatalysts, Phys. Chem. Chem. Phys. 12 (2010) 960–969.
[48] V. Latour, T. Pigot, M. Simon, H. Cardy, S. Lacombe, Photo-oxidation of di-n-butylsulfide by various electron transfer sensitizers in oxygenated acetonitrile, Photochem. Photobiol. Sci. 4 (2005) 221–229.
[49] C. Cantau, T. Pigot, R. Brown, P. Mocho, M.-T. Maurette, F. Benoit-Marqué, S. Lacombe, Photooxidation of dimethylsulfide in the gas phase: a comparison between TiO_2-silica and photosensitizer-silica based materials, Appl. Catal. B: Env. 65 (2006) 77–85.
[50] V. Latour, T. Pigot, P. Mocho, S. Blanc, S. Lacombe, Supported photosensitizers as new efficient materials for gas-phase photo-oxidation, Catal. Today 101 (2005) 359–367.
[51] D.T. Sawyer, J.S. Valentine, How super is superoxide, Acc. Chem. Res. 14 (1981) 393–400.